Electronic Supplementary Material (ESI) for Nanoscale.
This journal is © The Royal Society of Chemistry 2015

Supporting Information

Revealing Silent Vibration Modes of Nanomaterials by Detecting Anti-Stokes Hyper-Raman Scattering with Femtosecond Laser Pulses

Jianhua Zeng,[a] Lei Chen,[a] Qiaofeng Dai,[a] Sheng Lan*[a] and Shaolong Tie*[b]

SI-1 Sample structure and experimental setup

MoS_2 layers with different thicknesses were exfoliated on different substrates of SiO_2/Si, Au/SiO_2 and SiO_2-SnO_2/Ag/SiO_2, as schematically shown in Fig. S1(a). The color exhibited by a MoS_2 layer depends strongly on the thickness of the MoS_2 layer and the substrate used. The experimental setup used to characterize the nonlinear optical properties of the nanomaterials is schematically shown in Fig. S1(b). The fs laser pulses were reflected by a dichroic mirror and focused on the samples by using the objective lens of an inverted microscope. The nonlinear signals generated by the nanomaterials were collected by the same objective lens and directed to a spectrometer for analysis.

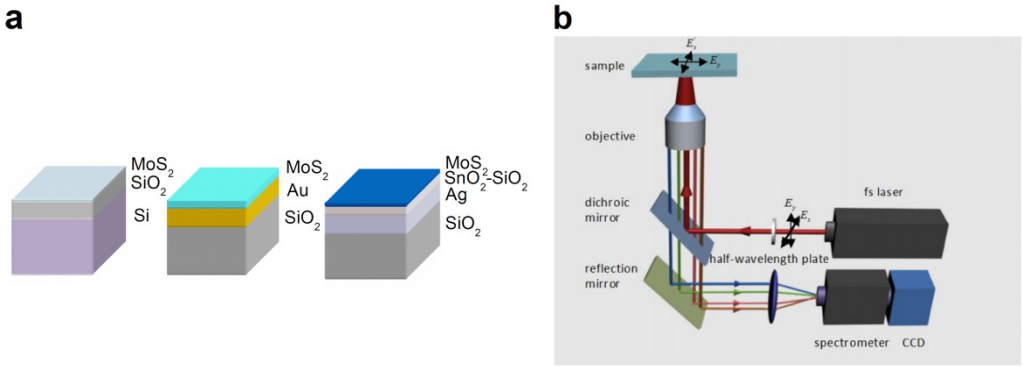

Fig. S1 (a) MoS_2 layers exfoliated on a SiO_2/Si，an Au/SiO_2 and a SiO_2- SnO_2/Ag/SiO_2 substrate. (b) Experimental setup used to characterize the nonlinear optical responses of the MoS_2 layers on the SiO_2/Si, Au/SiO_2 and SiO_2- SnO_2/Ag/SiO_2 substrate and other nanomaterials.

SI-2 Linear optical properties of MoS_2 layers on different substrates

The complex refractive index of MoS_2 used to calculate the reflection spectra of the MoS_2 layers on different substrates is shown in Fig. S2(a). The reflection spectra calculated for the 17 nm MoS_2 layer on the Au/SiO_2 substrate and the 9 nm MoS_2 layer on the SiO_2-SnO_2/Ag/SiO_2 substrate are presented in Fig. S2(b). The Chromaticity coordinates derived for the 17 nm-thick MoS_2 on the Au/SiO_2 substrate and the 9 nm-thick MoS_2 on the SiO_2-SnO_2/Ag/SiO_2 substrate based on their reflection spectra shown in Fig. S2 (b) are presented in Fig. S2(c). The Raman spectra measured for the 17 nm-thick MoS_2 on the Au/SiO_2 substrate and the 9 nm-thick MoS_2 on the SiO_2-SnO_2/Ag/SiO_2 substrate at an excitation wavelength of 514 nm are presented in Fig. S3(a). Two peaks located at 382.2 and 407.4 cm^{-1}, which are attributed to the in-plane (E^1_{2g}) and out-of-plane (A_{1g}) vibration modes, were clearly resolved in the Raman spectra. The MoS_2 layers were confirmed to be bulk material by the frequency difference between the two modes which is estimated to be 25.2 cm^{-1}.[S3] When the excitation power of the fs laser light exceeds a critical value, the ablation of the MoS_2 layer may occur, leading to the reduction in the thickness, as shown in Fig. 4(a). A change in both the SHG intensity and the film color was observed. In order to find out the physical origin for the change in SHG intensity and film color, we measured the Raman scattering spectra for the un-ablated and ablated areas of the 17 nm-thick MoS_2 layer on the Au/SiO_2 substrate, as

shown in Fig. S3(b). Except the signal intensity, we found no change in the Raman scattering peaks, indicating that the irradiation of fs laser pulses results in the ablation of MoS_2 rather than the 2H to 1T/T′ phase transition.

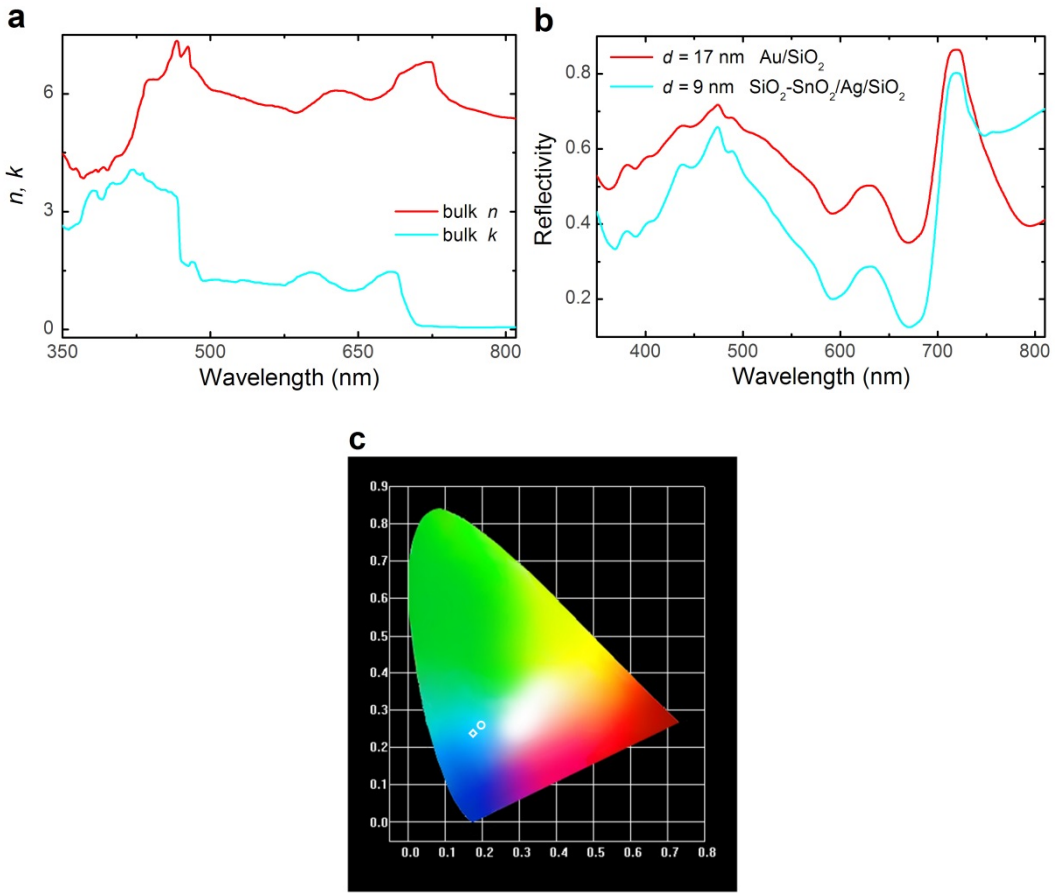

Fig. S2 (a) Complex refractive index of MoS_2 used in the calculation of the reflection spectra. (b) Reflection spectra calculated for the 17 nm-thick MoS_2 on the Au/SiO_2 substrate and the 9 nm-thick MoS_2 on the SiO_2-SnO_2/Ag/SiO_2 substrate. (c) Chromaticity coordinates derived for the 17 nm-thick MoS_2 on the Au/SiO_2 substrate (circle) and the 9 nm-thick MoS_2 on the SiO_2-SnO_2/Ag/SiO_2 substrate (rhomb) based on the reflection spectra shown in (b). Complex refractive indexes of Au, Ag, Si and SiO_2 used in the numerical simulations are based on Refs. S1 and S2.

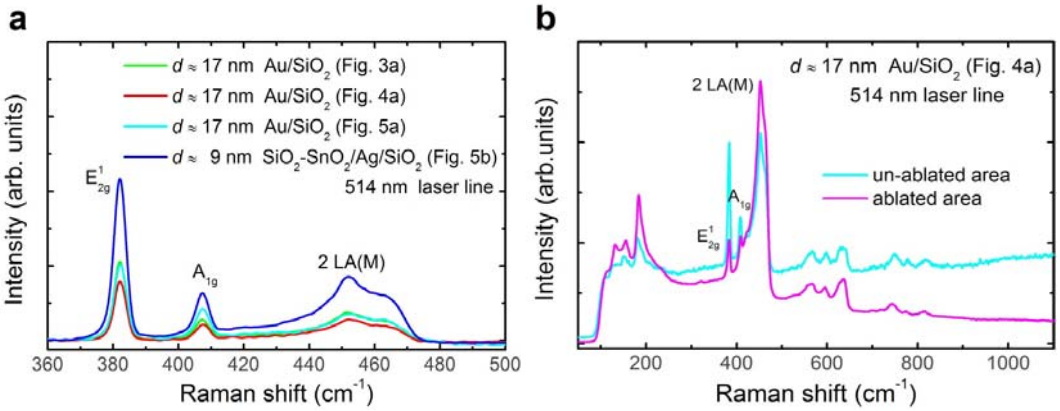

Fig. S3 (a) Raman scattering spectra measured at 514 nm for the 17 nm-thick MoS_2 layer on the Au/SiO_2 substrate shown in Figs. 3a, 4a and 5a and the 9 nm-thick MoS_2 layer on the SiO_2-SnO_2/Ag/SiO_2 substrate shown in Fig. 5b. (b) Raman scattering spectra measured at 514 nm for the un-ablated and ablated areas of the 17 nm-thick MoS_2 layer on the Au/SiO_2 substrate shown in Fig. 4a.

SI-3 Multiple Gaussian fitting of the hyper-Raman scattering spectra

In order to derive the frequencies or the Raman shifts of the vibration modes from the hyper-Raman scattering spectra, we employed multiple Gaussian fitting to decompose the hyper-Raman spectra measured for different nanomaterials, as shown in Fig. S4.

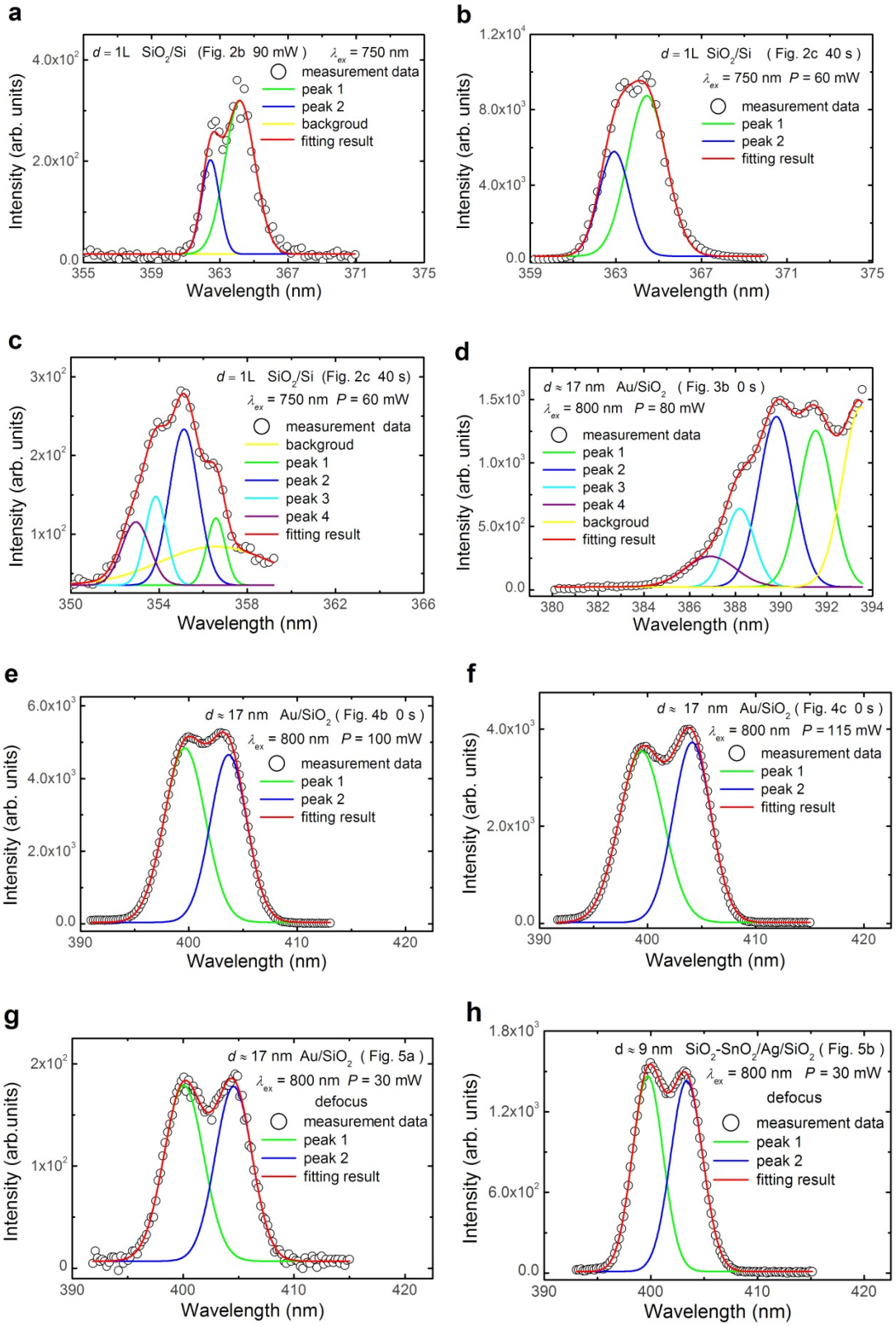

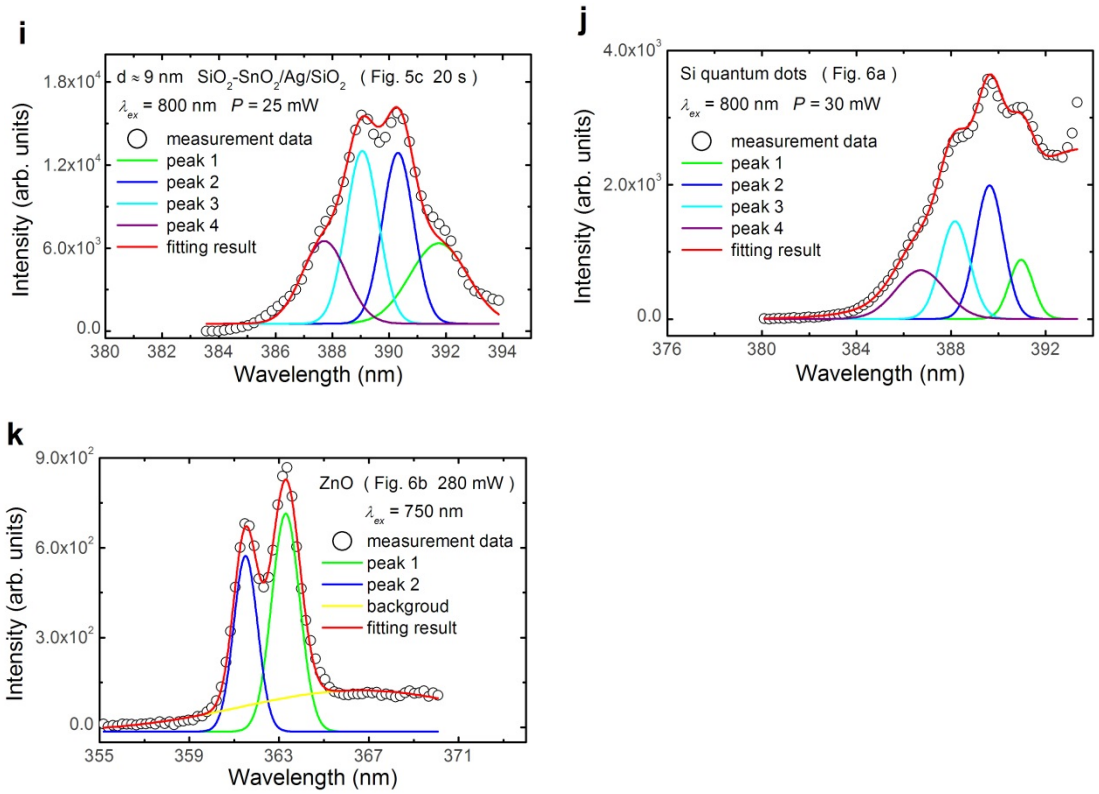

Fig. S4 Multiple Gaussian fitting of the hyper-Raman spectra measured for different nanomaterials. (a)-(c) Single-layer MoS_2 on the SiO_2/Si substrate (see Figs. 2b and 2c). (d)-(g) 17-nm-thick MoS_2 on the Au/SiO_2 substrate (see Figs. 3b, 4b, 4c and 5a). (h) and (i): 9-nm-thick MoS_2 on the SiO_2-SnO_2/Ag/SiO_2 substrate (see Figs. 5b and 5c). (j) Si QDs self-assembled into "coffee" rings (see Fig. 6a). (k) Cu-doped hollow ZnO NRs (see Fig. 6b). In each case, the circles are the measurement data while the red curve is the fitting result.

SI-4 Dependence of the SHG and hyper Raman intensities on the excitation power

In our experiments, we also measured the dependence of the SHG and anti-Stokes hyper-Raman scattering (AHRS) intensities on the excitation power for different nanomaterials and plotted the experimental data in a double logarithmic coordinate, as shown in Fig. S5. The slopes extracted by fitting the experimental data were found to be ~2.0, which is in good agreement with the second-order nature of the nonlinear optical processes.

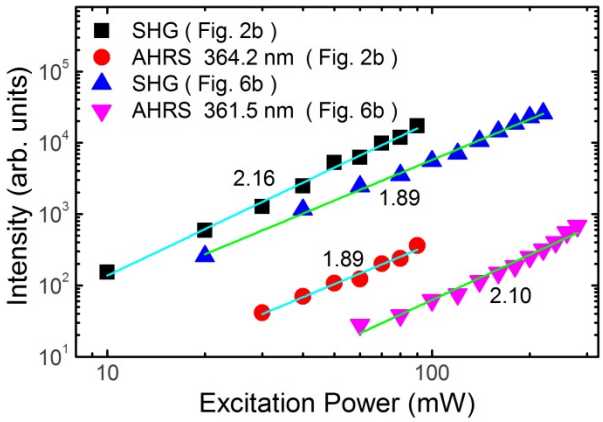

Fig. S5 Dependences of the SHG and anti-Stokes hyper-Raman scattering (AHRS) intensities on the excitation power, which are plotted in a double logarithmic coordinate, measured for different nanomaterials. The straight lines with indicated slopes show the fittings of the experimental data which are represented by squares, triangles and circles.

SI-5 Frequencies and Raman shifts of the hyper-Raman scattering observed in different nanomaterials

Based on the multiple Gaussian fittings of the hyper-Raman scattering spectra, we have derived the frequencies and Raman shifts of the vibration modes observed for different nanomaterials. The results are summarized in Tables S1 and S2.

Table S1 Wavelengths of the vibration modes derived by the multiple Gaussian fittings of the hyper-Raman spectra measured for different nanomaterials

Observed-peak positions (nm)						Sample, substrate	Fig.
λ_1	λ_2	λ_3	λ_4	λ_5	λ_6		
364.2	362.5					1L, SiO_2/Si	2b
364.5	362.9	356.6	355.1	353.9	352.9	1L, SiO_2/Si	2c
391.5	389.8	388.2	386.9			17 nm, Au/SiO_2	3b
399.6	403.7					17 nm, Au/SiO_2	4b
399.4	404.1					17 nm, Au/SiO_2	4c
400.1	404.6					17 nm, Au/SiO_2	5a
399.7	403.4					9 nm, SiO_2-SnO_2/Ag/SiO_2	5b
391.8	390.3	389.1	387.7			9 nm, SiO_2-SnO_2/Ag/SiO_2	5c
391.0	389.6	388.2	386.7			Si QDs	6a
363.3	361.5					Cu-doped ZnO NRs	6b

Table S2 Raman shifts of the vibration modes derived by the multiple Gaussian fittings of the hyper-Raman spectra measured for different nanomaterials

Observed peaks positions (cm^{-1})						Sample, substrate	Fig.
ω_1	ω_2	ω_3	ω_4	ω_5	ω_6		
-793.04	-923.4					1L, SiO_2/Si	2b
-771.94	-887.6	-1377.5	-1492.0	-1593.9	-1666.8	1L, SiO_2/Si	2c
-542.1	-654.8	-760.6	-845.8			17 nm, Au/SiO_2	3b
SHG	250.4					17 nm, Au/SiO_2	4b
SHG	290.6					17 nm, Au/SiO_2	4c
SHG	278.0					17 nm, Au/SiO_2	5a
SHG	225.8					9 nm, SiO_2-SnO_2/Ag/SiO_2	5b
-526.5	-620.0	-703.0	-791.8			9 nm, SiO_2-SnO_2/Ag/SiO_2	5c
-578.1	-666.0	-762.6	-858.5			Si QDs	6a
-858.8	-995.1					Cu-doped ZnO NRs	6b

References

S1 P. B. Johnson and R. W. Christy, *Phys. Rev. B*, 1972, **6**, 4370-4379.

S2 E. D. Palik, *Handbook of Optical Constants of Solids*, Academic, New York, 1985.

S3 H. Li, Q. Zhang, C. C. R. Yap, B. K. Tay, T. H. T. Edwin, A. Olivier and D. Baillargeat, *Adv. Funct. Mater.*, 2012, **22**, 1385-1390.